Characterizing Star-sawn Pattern–Produced and Orthogonally Glued Specimens of Southern Pine

Guangmei Cao Rubin Shmulsky Ming Liu
Edward D. Entsminger Brian K. Via Hui Wan

Abstract

In this study, triangular specimens of southern pine (*Pinus* spp.; SP) generated by a star-sawn process were characterized according to knots and deformation. SP specimens were used to understand the differences among glue-line combinations of radial-to-radial, radial-to-tangential, and tangential-to-tangential faces bonded with phenol resorcinol formaldehyde resin. The specimens were tested for shear strength, dimensional stability, wood failure, and delamination rate in accordance with ASTM D1037 and D2559 standards. Among the star-sawn triangular samples studied, bows in tangential-face sections occurred the most. The radial-face sections of SP triangular specimens had more knots but a much lesser degree of deformation than the tangential-face sections. The tangential-to-tangential face glue-line samples showed a lower shear strength, more wood failure, and a greater tendency of delamination and dimensional change, especially when subjected to wet conditions. Confocal microscopic pictures revealed that the tangential-to-tangential glue line showed a greater tendency of deformation in the earlywood part and helped to explain the reason for poor glue-line durability and low shear strength. This article revealed that the star-sawn–process generated wood radial-face samples were more stable than others tested and are perhaps a good alternative for massive panel manufacturing.

Cross-laminated timber (CLT) was first invented in Europe in the 1990s and has performed well as a building material (Espinoza et al. 2016). Considering the popularity of this topic worldwide, an increase in CLT production is projected (Brandner et al. 2016). CLT carries several advantages, such as being versatile toward more applications and having good dimensional stability, a reduced carbon footprint during the manufacturing process, and good aesthetics; its weight is lighter for a given strength compared to steel and concrete. However, the development of CLT in North America is still in its infancy.

A review of the literature reveals that CLT is typically limited to specific wood species for certain geographical areas. The softwood materials most commonly used for CLT in the north are spruce (*Picea* spp.), pine (*Pinus* spp.), fir (*Abies* spp.), and larch (*Larix* spp.). Hardwoods are less commonly used because the higher density and twisted wood grain may cause problems such as fracture, checking, and uneven shrinkage (Niemz and Sonderegger 2013), which affect the utilization of these hardwoods for CLT manufacturing. Currently, CLT manufacturing normally utilizes 5.08 by 10.16-cm or 5.08 by 15.24-cm lumber and a polyurethane adhesive. These materials are assembled and cold pressed in perpendicular adjacent layers to make CLT panels.

Because the log-to-lumber yield rate is often about 60 percent (Olufemi et al. 2012), the overall resource utilization efficiency in CLT manufacturing is lower than some other wood composites such as oriented strand board. Along with the relatively high costs of labor, operations, and the adhesive used, this yield rate keeps the cost of CLT relatively high (Buck et al. 2015).

It is well known that the dimensional stabilities of wood in the tangential and radial sections are different: normally,

The authors are, respectively, Graduate Student, Professor and Dept. Head, Graduate Student, and Research Associate, Dept. of Sustainable Bioproducts, Mississippi State Univ., Starkville (gc817@student.exchange.msstate.edu, rs26@msstate.edu, mingliu1204@gmail.com, ede37@msstate.edu); Regions Bank Professor of Forest Products, Director of the Forest Products Development Center, Auburn Univ., Auburn, Alabama (brianvia@auburn.edu); and Associate Professor, Dept. of Sustainable Bioproducts, Mississippi State Univ., Starkville (hw2@msstate.edu [corresponding author]). All authors are members of the Forest Products Society. This manuscript was published as journal article SB 936, Forest and Wildlife Research Center, Mississippi State Univ., Mississippi State. This paper was received for publication in July 2018. Article no. 18-00031.
©Forest Products Society 2019.
Forest Prod. J. 69(1):53–60.
doi:10.13073/FPJ-D-18-00031

http://prime-pdf-watermark.prime-prod.pubfactory.com/ | 2024-12-26

tangential shrinkage is about twice as great as radial (Simpson and TenWolde 1999). This results in greater dimensional change in plain/flat sawn lumber than in quarter-sawn lumber at the face direction of the lumber width, partially due to the ray cells' shrinkage/swelling in the radial direction and partially due to the discontinuation of shrinkage/swelling generated, for example, by quarter-sawn southern pine (SP) lumber. This affects the durability of the SP glue line. However, the advantage of a great dimensional stability of the radial section was not well exploited in normal engineered lumber production, due to the limitation of the flat sawn pattern during lumber manufacturing.

The ''star-sawn'' pattern uses a relatively new sawing method for wood (Sandberg and Holmberg 1996, 1998) and was developed by Sandberg (1996). It is similar to quarter sawn, which means the lumber or cant manufactured by this sawing pattern has growth rings at the angles of 45° to 90° to the wide surface of the board (Wiedenhoeft 2010, Hardwood Distributor's Association 2018). The star-sawn pattern process cuts through the center of a log and obtains triangle-shaped specimens. Since it contains heartwood, it has the potential to use a greater portion of a log. One key difference from a quarter-sawn cut pattern is that the star-sawn pattern has a cutting angle that can be changed to any desired angle instead of a fixed 90° angle, while the cut face plane is always perpendicular to wood growth ring. In addition, the generated triangular specimen has three surfaces that can be glued together once converted to glue-line elements: two radial surfaces and one tangential surface, which gives more flexibility in manufacturing.

There are, however, some barriers to applying star-sawn technology. First, it is slow compared to conventional sawmilling, based on the current star-sawn technology developed. Next, unlike rectangular lumber, the triangles from the star-sawn process have no market value and must be further processed into engineered lumber. Finally, special handling, drying, sorting, grading, machining, and assembling equipment would need to be designed and built in order to adopt this technology in any type of significant manner.

Because CLT adoption in North America is still under development, research on the fundaments of new manufacturing methods is necessary. In this article, we characterized the features of SP specimens generated by a star-sawn pattern and investigated the bonding performance of glue lines or bond lines made of radial- and tangential-face sections bonded with a phenol resorcinol formaldehyde (PRF) resin in accordance with ASTM standards.

Materials and Methods

Materials

Twenty-five pieces of SP logs with a diameter greater than 27.94 cm were donated by Weyerhaeuser Co. (Philadelphia, Mississippi). Triangular section specimens were cut from these logs. The triangular section specimens were then kiln-dried at the Mississippi State University Department of Sustainable Bioproducts Kiln Laboratory. After this, the kiln-dried specimens were measured for density and moisture content (MC). The features of SP are shown in Table 1. A commercial PRF adhesive was used and the features of the PRF adhesive are listed in Table 2.

Star-sawn process

The following process sequence was used in manufacturing the star-sawn triangles. First, debarked SP logs with 27.94- or 35.56-cm diameters were cut into 243.84-cm lengths. These logs were then star-sawn into equilateral-triangle section cants according to the process described in Figure 1. So this process generated six pieces of 243.84-cm-long equilateral-triangle section specimens with a side length <17.78 cm.

Log-to-lumber yield rate evaluation

In total, 150 pieces of triangular cants were produced from 25 pieces of SP logs. Based on the height and the length of a triangle, the volume of each triangular specimen was obtained with the following equation:

$$V = \frac{\sqrt{3}}{4} a^2 \times L \tag{1}$$

where

V = volume of a triangular specimen (m^3),
a = length of a triangular side (m), and
L = length of a triangular specimen (m).

Drying method

After application of the star-sawn procedure, the 150 pieces of triangular specimens were dried according to the schedule listed in Table 3. After drying, the MC of the cants were measured once a week until the average MC of all the cants reached 12 percent or below. Then the crook, bow, and twist of the dried specimens were measured and evaluated, to find the suitability of a piece of triangular specimen for gluing into engineered lumber.

Deformation and knot evaluation of wood specimens

During the evaluation process, the three surfaces of each kiln-dried triangular cant were marked and the degree of deformation of bow, crook, and twist were respectively measured according to the method described by Erickson

*Table 1.—Features of southern pine (*Pinus *spp.).*

Source	Weyerhaeuser, Mississippi
Density (kiln-dry) (kg/m^3)	618
MC (kiln-dry) (%)	8–15

Table 2.—Features of phenol resorcinol formaldehyde (PRF) adhesive.

Phenol resorcinol adhesive (Cascophen LT-75C)	100 parts
Hardener (Cascoset FM-282)	15–17 parts
Operational time at room temperature (21°C)	2.5 h
Viscosity	150–170 cPs
Clamp time (21°C–24°C)	9 h
Resin solid content (%)[a]	21

[a] At 6:1 PRF resin:hardener ratio.

http://prime-pdf-watermark.prime-prod.pubfactory.com/ | 2024-12-26

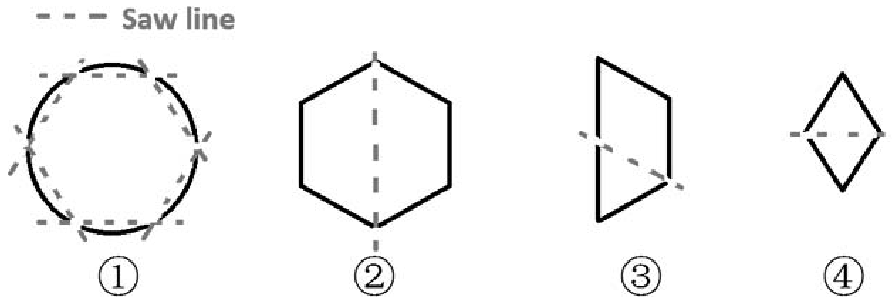

Figure 1.—Star-sawn sawing design and process.

Table 3.—Southern pine kiln drying schedule.

Time (h)	Dry bulb temperature (°C)[a]	Wet bulb temperature (°C)	Comments
0–12	Ramp up from 27–107	Ramp up from 24–57	Warm-up period, initial drying
10–16	107	57	Constant drying rate
16–18	96	49	Reduced temperature during drying to minimize surface checking
18–38	Ramp down from 96–79	Ramp down from 49–43	Drying rate decreasing as fiber saturation point approached
38			Stop kiln, hot check for moisture content
38–98	49	27	Continue drying and equalizing below the fiber saturation point

[a] Dry bulb temperature was recorded and the kiln was controlled on the exiting (cooler) side of the stack.

and Shmulsky (2005). A judgment of ''straight'' was assigned for future glue-line manufacturing preparation if any one of three surfaces of a piece of triangular specimen had the deformation equal to or smaller than 5 mm. During the measurement, if there were bow, crook, or twist that happened at the same face section, the most dominant one was recorded. The number of knots was recorded by visual observation.

Bonding performance evaluation

In order to find out if differences in different gluing methods exist and to reduce variation in measurements, end-matched defect-free SP wood stick samples with dimensions of 5.08 (width) by 1.27 cm (thickness) at varied lengths from the same log were planed true and selected. These glue-line samples were glued with radial-to-radial faces (RR), radial-to-tangential faces (RT), and tangential-to-tangential faces (TT) at a resin loading of 215.3 g/m^2 and cold pressed with a 16.6 kg·m torque via Black Brother Press (Black Bros. Co., Mendota, Illinois) for 24 hours. After cold pressing, the glued samples were divided into three groups of control, modified ASTM D1037-12 (ASTM International 2012a), and ASTM D2559-12 (ASTM International 2012b) test sets. The experimental design is shown in Table 4.

For the control samples, after conditioning at 21°C and a relative humidity of 42 percent for 2 weeks, an equilibrium MC of 8 percent was reached. The wood stick samples were cut and trimmed to a 4.2 by 2.4-cm bonding area for block shear testing (ASTM D1037-12). For the modified ASTM D1037 test, the wood stick samples were subjected to three wet–freeze–ovendry cycles, which were described previously (Wan et al. 2017). Briefly, for the wet exposure test, a weatherometer chamber was used. Inside the chamber, four nozzles sprayed tap water on the specimens at a rate of 6 to 8 kg/min until the MC of specimens reached at least 30 percent (above fiber saturation point), within about 12 hours. The freeze treatment consisted of placing the water-saturated samples in a freezer set at –22°C for 24 hours. After this, samples were oven dried at 103°C ± 2°C for 24 hours. This procedure was repeated three times. During the process, the dimensional changes of the wood stick samples were measured to obtain wood cross-section swell-rate data. After these three wet–freeze–ovendry cycles, the samples were conditioned to 8 percent MC in the conditioning chamber for 2 weeks and cut into block shear specimens with dimensions the same as the control block shear specimens. The wood failure and dimensional stability of RR, RT, and TT glue-line samples subjected to three wet–freeze–ovendry cycles were also evaluated.

As per the ASTM D2559-12 (ASTM International 2012b) test method, the wood stick samples were processed and delamination rates were measured at the end of the final drying step of the third cycle, with a gap filler of 0.008 cm.

Table 4.—Experimental design.

Glue face[a]	Treatment	Stick sample number	Shear block number
RR	Control	2	12
	ASTM D2559	2	11
	Modified ASTM D1037	2	22
RT	Control	2	12
	ASTM D2559	2	10
	Modified ASTM D1037	2	21
TT	Control	2	11
	ASTM D2559	2	11
	Modified ASTM D1037	2	22

[a] RR = radial-to-radial; TT = tangential-to-tangential; RT = radial-to-tangential.

http://prime-pdf-watermark.prime-prod.pubfactory.com/ | 2024-12-26

During this process, checks with depth less than 0.64 cm (1/4 in) or shorter than 2.54 cm (1 in) in length were not recorded. After water soaking and drying as described by the standard, all wood sticks were cut into block shear specimens with the same dimensions as the control samples and put into an environmental conditioning chamber for 2 weeks to reach a targeted 8 percent MC. Then they were tested for shear strength according to ASTM D1037-12 (ASTM International 2012a) at a loading rate of 0.6 mm/min, with at least 10 replicates.

Confocal microscope observation

The resin penetration of the control samples of three different wood section glue lines was observed using a Carl Zeiss Axiovert 200 M Inverted Research microscope at magnification = ×10, numerical aperture = 0.30, and working distance = 5.60 mm. The samples for confocal microscopy were prepared in the ammonia solution (NH_3 content at 28% to 30%) to soften the wood texture for 24 hours, then a single-edge prep razor blade was used to slice a sample to obtain a smooth surface for observation. Samples were placed on a glass slide when the confocal laser scanning was conducted.

Dimensional stability

The dimensional stability or the swell rate (RS) of wood glue-line specimens during three wet-freeze-ovendry cycle treatments was calculated by:

$$RS\ (\%) = (S_n - S_1)/S_1 \times 100\% \quad (2)$$

where

RS = swell rate (%),
S_1 = cross-section area before a treatment (m^2), and
S_n = cross-section area after each treatment (m^2).

Statistical analytical method

Data were analyzed by PROC GLM process in SAS software. The analysis of variance and comparison lines for least squares means were performed to tell whether the differences were significant or not at $\alpha = 0.05$.

Results and Discussion

Knot and deformation of triangular specimens

Generally, the green-log to triangular-specimen yield was between 73.7 and 77.5 percent, depending on log diameter. Normally, smaller logs tended to have a higher yield. This verified Sandberg's (1996) finding that the volume yield of timber with vertical annual rings in star-sawing was about 70 percent. After drying and being kept in the Mississippi State University Department of Sustainable Bioproducts Building 2 Wood Processing Laboratory for 3 weeks, the MC of the SP triangular samples was below 12 percent. As mentioned before, a piece of triangular sample had three surfaces (one tangential surface and two radial surfaces) which could be applied for gluing. The percentage of knot, crook, bow, and twist of each face section of the specimen is listed in Table 5.

Although the radial-face section tended to have more knots than the tangential-face section (Table 5), the percentage of bow of the radial-face section was much lower than that of the tangential-face section. The percentage of crook was similar between both radial- and tangential-face sections. Radial-face sections had much more twist than tangential-face sections.

Table 5.—Deformation and knot information of the triangular specimens.

	Radial[a]	Tangential
Knot (%)	42.0	31.3
Bow (%)	5.0	38.7
Crook (%)	4.0	6.7
Twist (%)	28.0	6.7

[a] Radial face data were the average of two readings.

The extent of deformation at the tangential-face section was significantly greater than that at the radial-face sections (Table 6). The extent of deformation at the two radial-face sections was not the same, but the difference was not significant ($\alpha = 0.05$). This indicates that during the process of making a glue line with SP, using the radial-face section as the glued face will be a more efficient resource utilization, since a radial-face section is flatter than a tangential-face section and planing a true radial face will generate much less waste, within the dimensions of triangular specimen used. It also indicates that once one selects the radial-face section as the gluing face, different radial faces will not make any difference in the glue-line manufacturing.

Based on differences in the frequency or percentage of knots and the degree of deformation that occurred within the tangential- and radial-face sections, to reduce waste, one should use the radial-face section of the specimens for gluing two pieces of triangular specimens. This finding was based on the data generated from 150 pieces of triangular cant at 243.8-cm length.

Shear strength of SP glue lines

The RT-face section glue line showed the highest shear strength of the control (dry) sample group and of the ASTM D1037-12 (ASTM International 2012a) test group (Fig. 2); the RR one had the highest shear strength of the ASTM D2559-12 (ASTM International 2012b) test group, though none of the differences between RR and RT in either group were significant. The TT-face section group did not show a high shear strength among any of the test groups. In the control group, the TT-face section resulted in significantly lower shear strength than RR and RT. This shows that the TT-face section glue line was not the best glue pattern or design for the glue line or for CLT/massive timber manufacturing. This verified the findings by Liu et al.

Table 6.—A comparison for extent of deformation at different wood sections.

Comparison lines for LS mean[a]		
Extent of deformation (mm)	Orientation	LS mean rank[b]
10.76	Tangential	A
0.82	Radial 1	B
0.48	Radial 2	B

[a] LS = least squares.
[b] LS means with the same letter are not significantly different.

http://prime-pdf-watermark.prime-prod.pubfactory.com/ | 2024-12-26

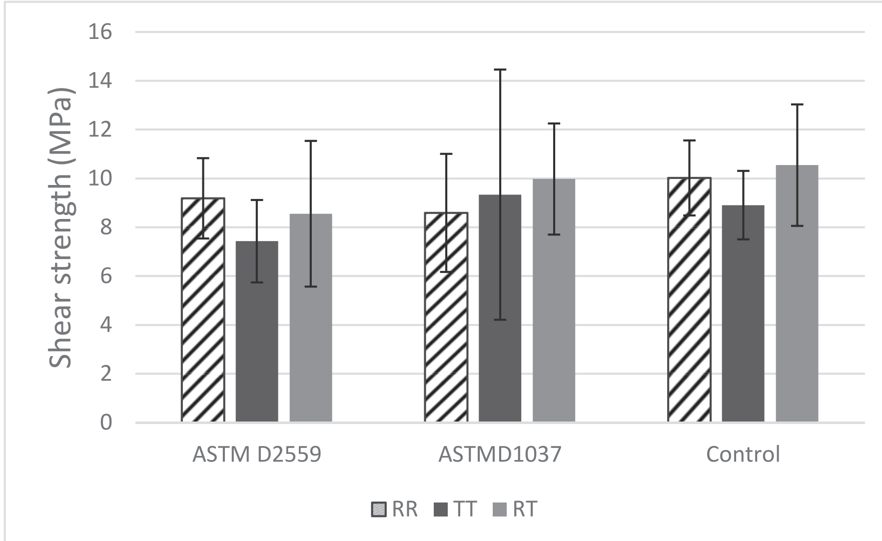

Figure 2.—Shear strength of southern pine glue lines. RR = radial-to-radial glue line; TT = tangential-to-tangential glue line; RT = radial-to-tangential glue line.

(2017) that at a specific gravity of 0.64, the SP RR glue line had a higher shear strength than the TT one.

Wood failure of SP glue lines

Wood failure of a glue line was defined as the ratio of exposed wood to the whole area in the fracture zone of a glue line (Frihart and Hunt 2010). The TT glue lines showed a relatively higher wood failure than any other glue lines among three tests (Fig. 3), but this was not significant. However, when compared to shear strength (Fig. 2), in most cases, the TT glue line resulted in lower shear strengths.

This finding again challenges the traditional concept in the wood adhesives industry that adhesive quality is evaluated together with wood failure as an important reference: the higher the shear strength, the more wood failure that occurs. Our test results indicate that a higher shear strength did not necessary yield a higher wood failure. Further research is needed to verify this finding.

Dimensional stability

The dimensional stability results are shown in Figure 4. It shows that when glue lines were subject to a wet–freeze–ovendry cycle, the glue lines of the different sets responded differently. The RR- and RT-face section glue lines showed a relatively stable tendency, while the TT group resulted in a wider fluctuation in dimension change when subjected to a cyclical wet–freeze–ovendry process. Based on this, the TT glue pattern appeared not as dimensionally stable as the RR and RT glue patterns, which also helped to

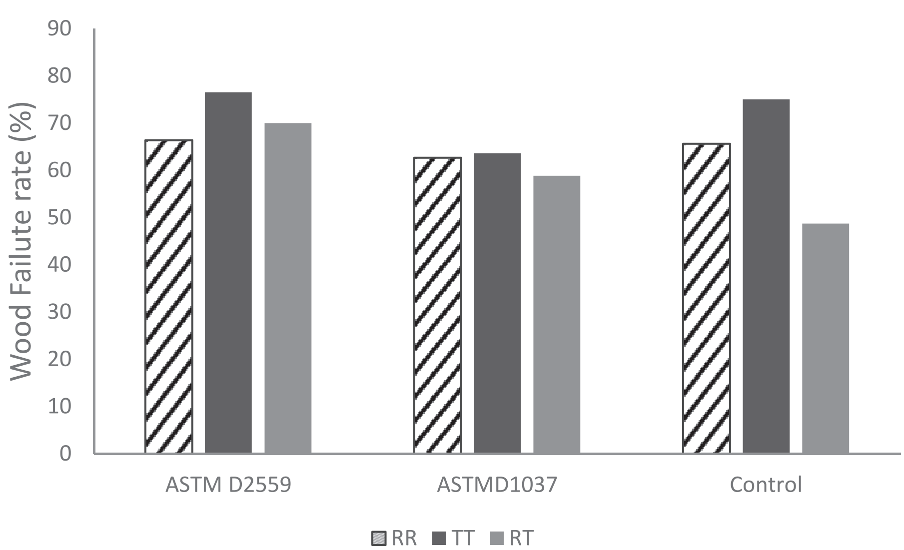

Figure 3.—Wood failure mean for each group. RR = radial-to-radial glue line; TT = tangential-to-tangential glue line; RT = radial-to-tangential glue line.

http://prime-pdf-watermark.prime-prod.pubfactory.com/ | 2024-12-26

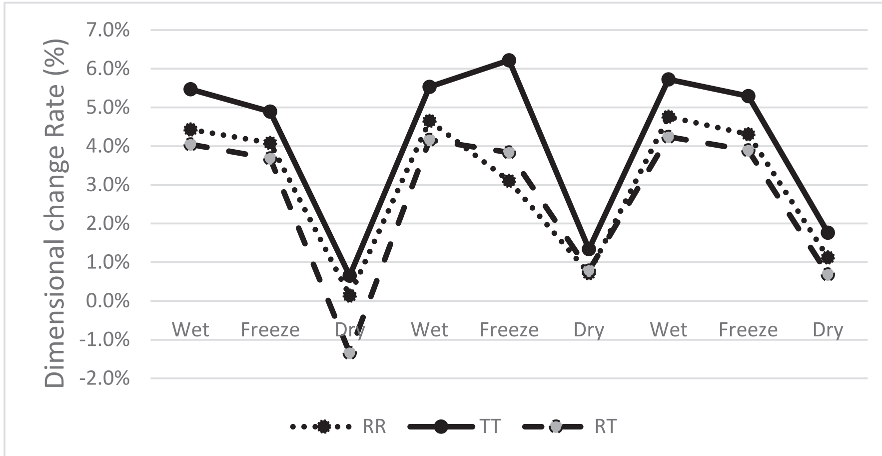

Figure 4.—Section dimensional change rate of the tested samples. RR = radial-to-radial glue line; TT = tangential-to-tangential glue line; RT = radial-to-tangential glue line.

explain the fact that TT section glue lines had a lower shear strength than those of RR and RT sections. The greater deformation stress of the wood elements of the TT glue line weakened the bonding of the TT glue line. However, since the dimensional stability data were obtained from an average of two replicates, further research is needed to verify this finding.

Delamination rate

The delamination rate after conditioning in accordance with ASTM D2559-12 (ASTM International 2012b) is shown in Figure 5. This figure indicates that the RT group had the lowest delamination rate of 24 percent and the RR group had a delamination rate of 33 percent. The TT group had the highest delamination rate of 58 percent. This also helped to explain the lower shear strength (Fig. 3) and dimensional stability (Fig. 4) of the TT glue line. Since delamination rate data were obtained from an average of two replicates, further research is needed to verify this finding.

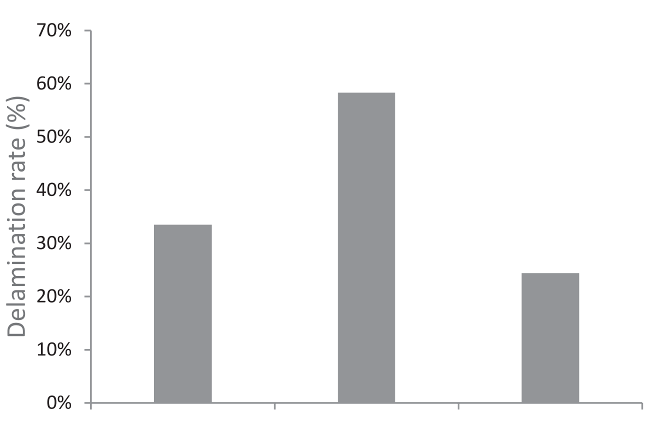

Figure 5.—Delamination rate of southern pine glue lines. RR = radial-to-radial glue line; TT = tangential-to-tangential glue line; RT = radial-to-tangential glue line.

Confocal microscopic figures

The confocal pictures of different glue-line zones are shown (Figs. 6, 7, and 8). It is evident that under the same resin loading and press conditions, the RR and RT glue lines resulted in a thick glue line, especially when earlywood was involved. The TT glue lines resulted in a more obvious deformation of earlywood (Fig. 8). This thick glue line and greater amount of resin in RR and RT glue lines (Figs. 6 and 7) had two functions: to hold wood together and to prevent wood elements from moving, especially when they were subjected to moisture change. The deformed earlywood elements in the TT glue line may have a greater tendency to restore the original shape when subjected to moisture changes, especially at a thin glue line. All these further

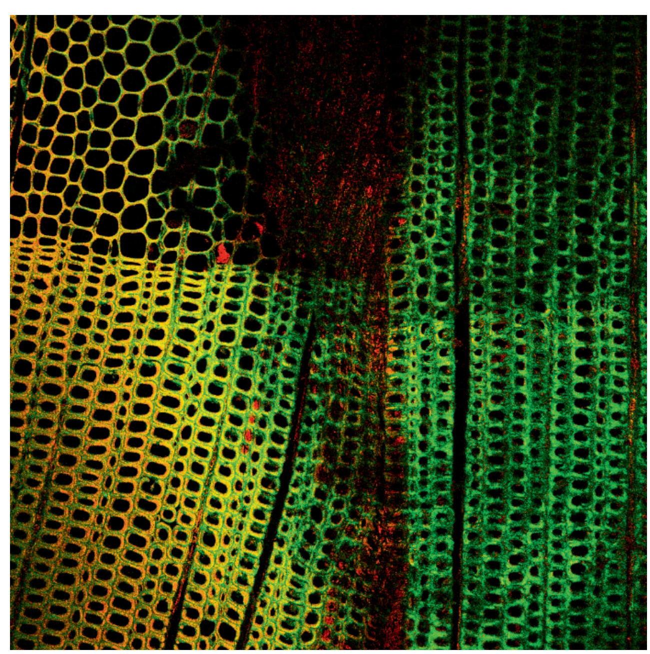

Figure 6.—Confocal picture of radial-to-radial sample glue line (×10). Resin in red.

http://prime-pdf-watermark.prime-prod.pubfactory.com/ | 2024-12-26

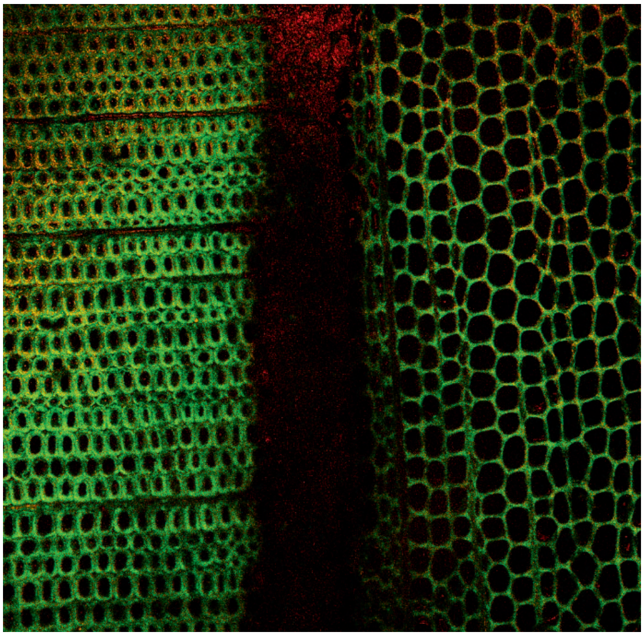

Figure 7.—Confocal picture of radial-to-tangential sample glue line (×10). Resin in red.

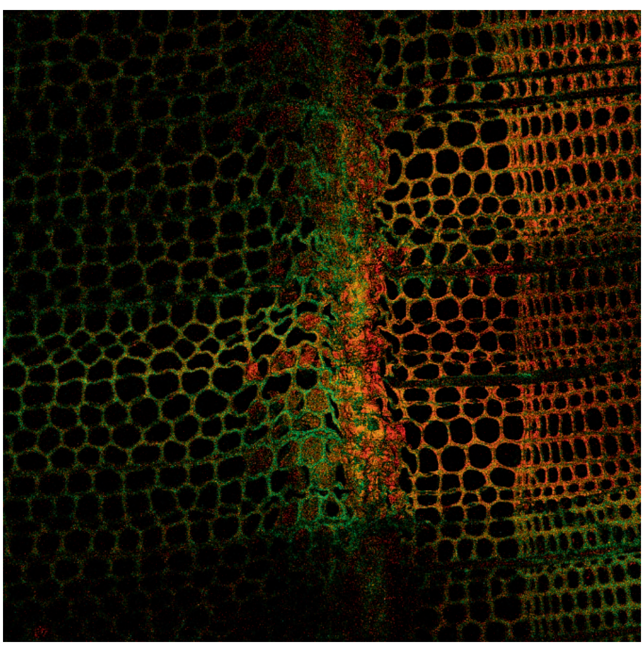

Figure 8.—Confocal picture of tangential-to-tangential sample glue line (×10). Resin in red.

explained why the RR and RT types of glue line had high shear strength, better dimensional stability, and less delamination than the TT-face section glue line. Further experimentation is necessary to verify this finding.

Conclusions

In this study, SP triangular specimens produced via the star-sawn process were characterized based on the frequency of surface knot and wood bow, crook, and twist. Radial and tangential wood face sections of the SP specimens were glued at the RR-, RT-, and TT-face section glue-line combinations with a commercial PRF resin. The specimens were tested for shear strength, wood failure, dimensional stability, and delamination rate in accordance with ASTM D1037 and D2559 (ASTM International 2012a, 2012b). Among the star-sawn specimens studied, deformation of wood elements most occurred in the formation of bows in the tangential-face section. The radial-face sections of the SP triangular specimens had more knots and much less deformation than the tangential-face section, and were more suitable for glue-line operations. The TT-face section glue line did not show a greater shear strength, and had more wood failures and a greater tendency of delamination than RR and RT glue lines. Confocal microscopic pictures revealed that the TT glue line showed a great tendency of cell collapse, which mainly happened in the earlywood section and explained a poor bond strength and poor glue-line durability of TT glue lines, especially after being subjected to wet conditions. From wood deformation and glue-line performance, this article revealed that the star-sawn process generated a stable and less deformed radial face section wood element for glue lines, which may be good for future massive panel manufacturing.

Acknowledgments

This research was funded by a grant from the USDA Forest Service Wood Innovations Program. This institution is an equal opportunity provider. The authors wanted to express their thanks to Professor D. Sandberg at Luleå University of Technology of Sweden for providing information on the star-sawing pattern.

Literature Cited

ASTM International. 2012a. Standard test methods for evaluating properties of wood-base fiber and particle panel materials. ASTM D1037-12. https://doi.org/10.1520/D1037-12. Accessed March 3, 2019.

ASTM International. 2012b. Standard specification for adhesives for bonded structural wood products for use under exterior exposure conditions. ASTM D2559-12. https://doi.org/10.1520/D2559-12AE01. Accessed March 3, 2019.

Brandner, R., G. Flatscher, A. Ringhofer, G. Schickhofer, and A. Thiel. 2016. Cross laminated timber (CLT): Overview and development. *Eur. J. Wood Wood Prod*. 74(3):331–351.

Buck, D., X.-D. (A.) Wang, O. Hagman, and A. Gustafsson. 2015. Comparison of different assembling techniques regarding cost, durability, and ecology—A survey of multi-layer wooden panel assembly load-bearing construction elements. *Bioresources* 10(4):8378–8396. DOI:10.15376/biores.10.4.8378-8396

Erickson, R. W. and R. Shmulsky. 2005. Warp reduction of red pine two-by-fours via restrained drying. *Forest Prod. J.* 55(9):84–86.

Espinoza, O., M. M. Laguarda, V. Trujillo, and U. Buehlmann. 2016. Cross-laminated timber: Status and research needs in Europe. *Bioresources* 11(1):281–295.

Frihart, C. R. and C. G. Hunt. 2010. Chapter 10: Adhesives with wood materials bond formation and performance. *In:* Wood Handbook—Wood as an Engineering Material. General Technical Report FPL-GTR-190. USDA Forest Service, Forest Products Laboratory, Madison, Wisconsin. pp. 10-1–10-24.

Hardwood Distributor's Association. 2018. What is the difference between quarter sawn, rift sawn and plain sawn lumber? http://www.hardwooddistributors.org/blog/postings/what-is-the-difference-between-quarter-sawn-rift-sawn-and-plain-sawn-lumber/. Accessed August 16, 2018.

Liu, M., Y. Q. Wu, and H. Wan. 2017. A new concept of wood bonding design for strength enhanced southern yellow pine wood products. *Construction Building Mater*. 157(2017):694–699.

Niemz, P. and W. Sonderegger. 2013. Cross laminated timber—

http://prime-pdf-watermark.prime-prod.pubfactory.com/ | 2024-12-26

Properties and use for building purposes: A review from the experience of Swiss researchers. *Pro Ligno* 9(1):3–21.

Olufemi, B., J. O. Akindeni, and S. O. Olaniran. 2012. Lumber recovery efficiency among selected sawmills in Akure, Nigeria. *Drvna Industrija: Znanstveni Časopis Za Pitanja Drvne Tehnologije* 63(1):15–18.

Sandberg, D. 1996. Radially sawn timber. Star-sawing—A new method for producing timber with vertical annual rings. *Holz Roh- Werkst*. 54(3):145–151.

Sandberg, D. and H. Holmberg. 1996. Radially sawn timber: Knots-number, type and size in star-sawn triangular profiles of pine (Pinus silvestris L) and spruce (Picea abies Karst). *Holz Roh- Werkst*. 54(6):369–376.

Sandberg, D. and H. Holmberg. 1998. Radially sawn timber. Gluing of star-sawn triangular profiles into form-stable products with vertical annual rings. *Eur. J. Wood Wood Prod*. 56(3):171–177.

Simpson, W. and A. TenWolde. 1999. Chapter 3: Physical properties and moisture relations of wood. *In:* Wood Handbook – Wood as an Engineering Material. General Technical Report FPL-GTR-113. USDA Forest Service, Forest Products Laboratory, Madison, Wisconsin. pp. 3–8.

Wan, H., J. Dahlen, A. Mao, L. Sites, A. Rowlen, G. Miller, B. McClendon, M. Liu, and D. Nicholas. 2017. Evaluation of the performance of composite wood decking bonded with phenol resorcinol formaldehyde and polyurethane adhesives after accelerated aging tests. *Forest Prod. J*. 67(1/2):112–119.

Wiedenhoeft, A. 2010. Chapter 3: Structure and function of wood. *In:* Wood Handbook—Wood as an Engineering Material. General Technical Report FPL-GTR-190. USDA Forest Service, Forest Products Laboratory, Madison, Wisconsin. pp. 3-1–3-18.

http://prime-pdf-watermark.prime-prod.pubfactory.com/ | 2024-12-26